






Prognostic value of right ventricular global longitudinal strain in patients with immunoglobulin light-chain cardiac amyloidosis

Hiroki Usuku ^{1,2,3}, Eiichiro Yamamoto^{2,3,*}, Daisuke Sueta ^{2,3}, Momoko Noguchi¹, Tomohiro Fujisaki^{2,3}, Koichi Egashira^{2,3}, Fumi Oike^{2,3}, Koichiro Fujisue ^{2,3}, Shinsuke Hanatani ^{2,3}, Yuichiro Arima ^{2,3}, Seiji Takashio ^{2,3}, Yawara Kawano⁴, Seitaro Oda ⁵, Hiroaki Kawano^{2,3}, Kenichi Matsushita ^{2,3,6}, Mitsuharu Ueda ^{3,7}, Hirotaka Matsui⁸, Masao Matsuoka⁴, and Kenichi Tsujita ^{2,3}

¹Department of Laboratory Medicine, Kumamoto University Hospital, 1-1-1 Honjo, Chuo-ku, Kumamoto 860-8556, Japan; ²Department of Cardiovascular Medicine, Graduate School of Medical Sciences, Kumamoto University, 1-1-1 Honjo, Chuo-ku, Kumamoto 860-8556, Japan; ³Center of Metabolic Regulation of Healthy Aging, Kumamoto University Faculty of Life Sciences, 1-1-1 Honjo, Chuo-ku, Kumamoto 860-8556, Japan; ⁴Department of Hematology, Rheumatology, and Infectious Diseases, Graduate School of Medical Science, Kumamoto University, 1-1-1 Honjo, Chuo-ku, Kumamoto 860-8556, Japan; ⁵Department of Diagnostic Radiology, Faculty of Life Sciences, Kumamoto University, 1-1-1 Honjo, Chuo-ku, Kumamoto 860-8556, Japan; ⁶Division of Advanced Cardiovascular Therapeutics, Kumamoto University Hospital, 1-1-1 Honjo, Chuo-ku, Kumamoto 860-8556, Japan; ⁷Department of Neurology, Graduate School of Medical Sciences, Kumamoto University, 1-1-1 Honjo, Chuo-ku, Kumamoto 860-8556, Japan; and ⁸Department of Molecular Laboratory Medicine, Faculty of Life Sciences, Kumamoto University, 1-1-1 Honjo, Chuo-ku, Kumamoto 860-8556, Japan

Received 28 March 2023; revised 25 April 2023; accepted 28 April 2023; online publish-ahead-of-print 9 May 2023

Handling Editor: Frank A. Flachskampf

Aims

Left ventricular (LV) global longitudinal strain (GLS) (LV-GLS) is a strong and independent predictor of outcomes in patients with immunoglobulin light-chain (AL) cardiac amyloidosis. This study was performed to investigate whether right ventricular (RV) GLS (RV-GLS) provides prognostic information in patients with AL amyloidosis.

Methods and results

Among 74 patients who were diagnosed with AL cardiac amyloidosis at Kumamoto University Hospital from December 2005 to December 2022, 65 patients who had enough information for two-dimensional speckle tracking imaging and did not receive chemotherapy before the diagnosis of cardiac amyloidosis were retrospectively analysed. During a median follow-up of 359 days, 29 deaths occurred. In two-dimensional echocardiographic findings, LV-GLS, left atrium reservoir strain (LASr), and RV-GLS were significantly lower in the all-cause death group than in the survival group (LV-GLS: 8.9 ± 4.2 vs. 11.7 ± 3.9 , $P < 0.01$; LASr: 9.06 ± 7.28 vs. 14.09 ± 8.32 , $P < 0.05$; RV-GLS: 12.0 ± 5.1 vs. 16.8 ± 4.0 , $P < 0.01$). Multivariable Cox proportional hazard analysis showed RV-GLS was significantly and independently associated with all-cause death in patients with AL cardiac amyloidosis (hazard ratio 0.85; 95% confidence interval, 0.77–0.94; $P < 0.01$). Receiver operating characteristic analysis showed that the area under the curve of RV-GLS for all-cause death was 0.774 and that the best cut-off value of RV-GLS was 14.5% (sensitivity, 75%; specificity, 72%). In the Kaplan–Meier analysis, patients with AL cardiac amyloidosis who had low RV-GLS ($<14.5\%$) had a significantly higher probability of all-cause death ($P < 0.01$).

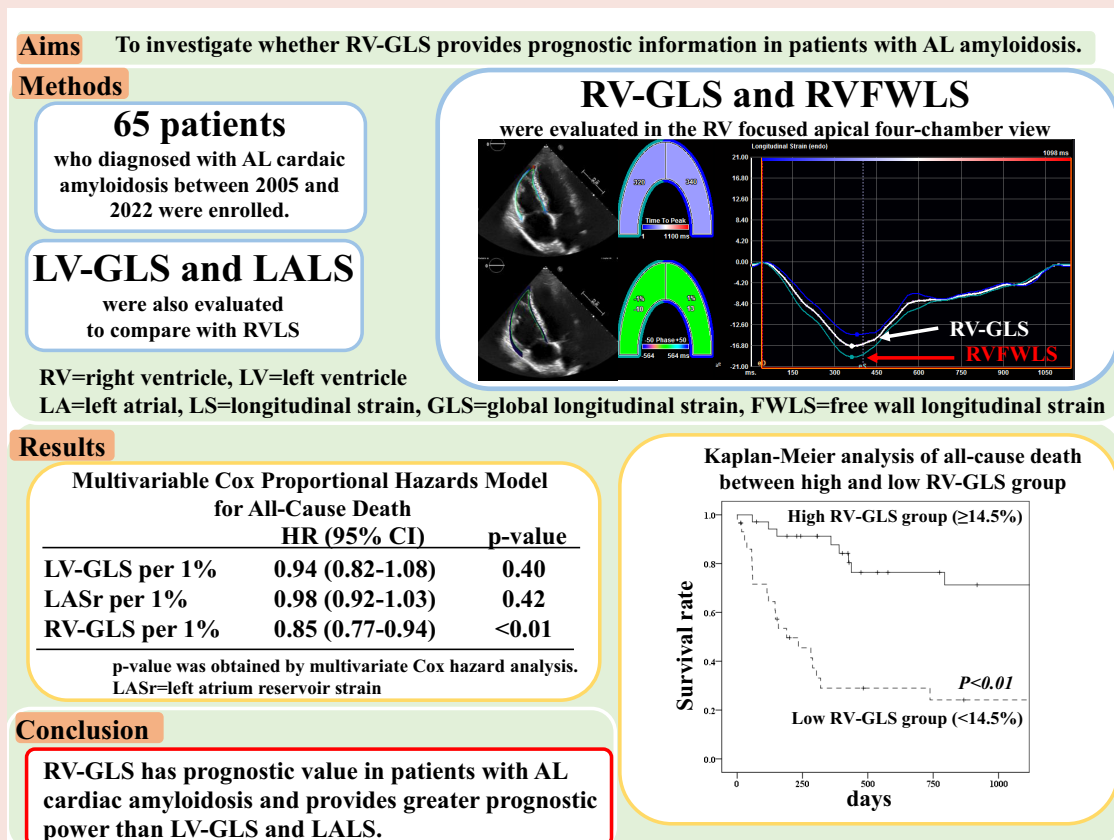
* Corresponding author. Tel: +81-96-373-5175, Fax: +81-96-362-3256, Email: eyamamo@kumamoto-u.ac.jp

© The Author(s) 2023. Published by Oxford University Press on behalf of the European Society of Cardiology.

This is an Open Access article distributed under the terms of the Creative Commons Attribution-NonCommercial License (<https://creativecommons.org/licenses/by-nc/4.0/>), which permits non-commercial re-use, distribution, and reproduction in any medium, provided the original work is properly cited. For commercial re-use, please contact journals.permissions@oup.com

Conclusion RV-GLS has prognostic value in patients with AL cardiac amyloidosis and provides greater prognostic power than LV-GLS and LASr.

Graphical Abstract



Keywords Immunoglobulin light-chain cardiac amyloidosis • Two-dimensional speckle tracking echocardiography • Right ventricular global longitudinal strain

Introduction

Amyloid cardiomyopathy is a clinical disorder in which interstitial deposition of amyloid fibrils causes morphological and functional abnormalities of the heart.¹ Amyloid cardiomyopathy is divided into three main types: immunoglobulin light-chain (AL) amyloidosis, mutant transthyretin amyloidosis, and wild-type transthyretin amyloidosis.¹ AL amyloidosis is a multisystem disease caused by the deposition of amyloid fibrils in organ tissues, and it arises from misfolded light chains most commonly produced by clonal expansion of monoclonal plasma cells.² Cardiac involvement has been noted in approximately 70% of patients with AL amyloidosis^{3,4} and is the primary driver of death in these patients.⁵

Myocardial amyloid deposition in cardiac tissues causes dysfunction through architectural damages as well as through direct myocardial toxicity and oxidative damage by amyloidogenic light chains.⁶ Echocardiographic findings provide diagnostic and prognostic information in patients with AL amyloidosis suspected of having cardiac

involvement.^{7,8} The hallmarks of amyloid cardiomyopathy on transthoracic echocardiography (TTE) are increased left ventricular (LV) thickness, left atrial (LA) enlargement, reduced systolic and diastolic LV function, and LV apical sparing.^{7,9,10} Additionally, amyloid can infiltrate virtually all cardiac chambers, including the right ventricle (RV).¹¹ Therefore, RV dysfunction is also a common finding in patients with amyloid cardiomyopathy.^{11,12} Two-dimensional strain analysis based on speckle-tracking echocardiography has recently been used to detect myocardial deformation.¹³ We previously reported the usefulness of RV longitudinal strain (LS) (RVLS) to predict cardiovascular events in patients with transthyretin amyloid cardiomyopathy.¹⁴ To our knowledge, however, few reports have focused on the usefulness of RVLS as a predictive factor in patients with AL amyloidosis compared with classical prognostic factors and other echocardiographic factors.

Thus, we hypothesized that RVLS estimated by two-dimensional speckle-tracking echocardiography in patients with AL amyloidosis might be an effective predictor of survival. We therefore investigated whether RVLS provides prognostic information in patients with AL amyloidosis.

Methods

Study population

In total, 74 patients were diagnosed with AL cardiac amyloidosis at Kumamoto University Hospital from January 2005 to January 2022. Of these patients, eight were excluded because they had no transthoracic echocardiography data at diagnosis or had insufficient two-dimensional speckle-tracking echocardiography data. In addition, one patient was excluded because he had already received chemotherapy before diagnosis of cardiac amyloidosis. The remaining 65 patients diagnosed with AL cardiac amyloidosis were enrolled in this study (Figure 1). Baseline clinical characteristics and electrocardiographic and echocardiographic data at diagnosis were obtained while the patients were clinically stable.

This study conformed to the principles outlined in the Declaration of Helsinki. It was approved by the institutional review board and ethics

committee of Kumamoto University (No. 1588). The requirement for informed consent was waived because of the low-risk nature of this retrospective study and the inability to obtain consent directly from all patients. Instead, we extensively announced this study protocol at Kumamoto University Hospital and on our website (<http://www2.kuh.kumamoto-u.ac.jp/tyuokensabu/index.html>) and gave patients the opportunity to withdraw from the study.

Diagnosis of AL cardiac amyloidosis

The diagnosis of amyloid deposition was based on Congo red staining and apple-green birefringence visualized with cross-polarized light microscopy in biopsied tissue samples. AL amyloidosis was diagnosed based on positive staining for immunoglobulin light chains by immunohistochemical staining. We diagnosed cardiac amyloidosis when amyloid deposition was observed in the myocardium, typical findings were observed on cardiac magnetic resonance imaging (CMR) (e.g. LV subendocardial late gadolinium enhancement or significantly elevated native T1 and extracellular volume fraction values), and/or a thickened LV wall was observed by cardiac echocardiography [interventricular septal thickness at end-diastole (IVSTd) of >12 mm] according to 2022 European Society of Cardiology cardio-oncology guidelines.¹⁵

Survival staging system

We evaluated survival staging as an objective prognostic indicator. Because Lillness *et al.*¹⁶ created a survival staging system using B-type natriuretic peptide (BNP) and cardiac troponin T (hs-cTnT), we separated enrolled patients into four groups (stages I, II, IIIa, and IIIb) as the reported cut-off points: stage I, both BNP and high-sensitivity cardiac troponin T (hs-cTnT) were lower than cut-off point (BNP = 81 pg/mL, hs-cTnT = 0.035 ng/mL), stage II: BNP or hs-cTnT were higher than the cut-off point, stage III: both BNP and hs-cTnT were higher than the cut-off point. Patients in stage III were also separated according to the BNP levels: stage IIIa, BNP ≤ 700 pg/mL; stage IIIb, BNP > 700 pg/mL.

74 patients diagnosed with cardiac AL amyloidosis between January 2005 and January 2022

8 patients who did not undergo a TTE examination at diagnosis or had insufficient information for two-dimensional speckle tracking echocardiography.
1 patient who had already received chemotherapy before diagnosis of cardiac amyloidosis.

65 patients with cardiac AL amyloidosis were enrolled in this study

Figure 1 Study flow chart detailing the inclusion and exclusion criteria for the study patients. AL amyloidosis, immunoglobulin light-chain amyloidosis; TTE, transthoracic echocardiography.

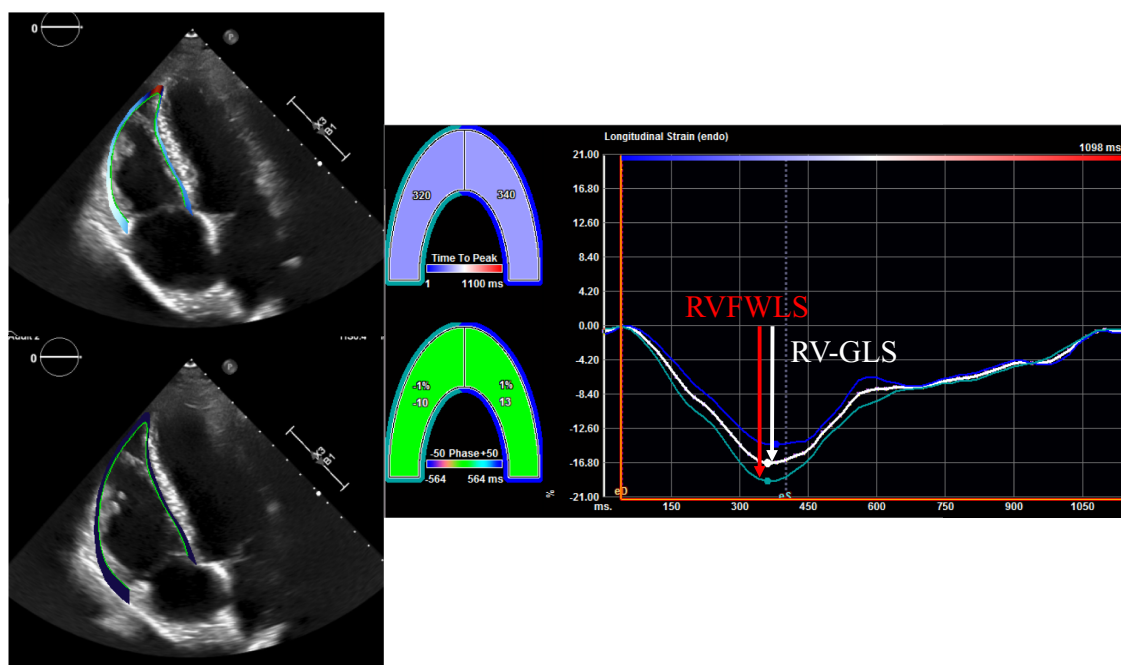


Figure 2 Representative example of right ventricular global longitudinal strain (white arrow) and right ventricular free wall longitudinal strain (red arrow). The peak longitudinal strain for right ventricular free wall and septal wall were averaged to provide right ventricular global longitudinal strain.

Table 1 Clinical characteristics between all-cause death group and event-free group

	Event-free group (n = 36)	All-cause death group (n = 29)	P-value
Baseline clinical characteristics			
Age, years	66.0 ± 9.8	69.9 ± 8.9	0.10
Male sex, n (%)	22 (61)	19 (66)	0.71
Body mass index, kg/m ²	22.7 ± 4.1	21.5 ± 3.3	0.18
Past medical history			
Hypertension, n (%)	17 (47)	7 (24)	0.06
Diabetes mellitus, n (%)	5 (14)	2 (7)	0.37
Dyslipidaemia, n (%)	9 (25)	5 (17)	0.45
Current smoking, n (%)	2 (6)	1 (3)	0.71
Atrial fibrillation, n (%)	5 (14)	5 (17)	0.71
ICD, n (%)	3 (8)	2 (7)	0.83
Pacemaker, n (%)	4 (11)	5 (17)	0.48
Stage I, n (%)	4/32 (13)	3/27 (11)	0.87
Stage II, n (%)	9/32 (28)	2/27 (7)	<0.05
Stage III, n (%)	19/32 (59)	22/27 (81)	0.07
Stage IIIa, n (%)	17/32 (53)	9/27 (33)	0.13
Stage IIIb, n (%)	2/32 (6)	13/27 (48)	<0.01
Systolic blood pressure, mmHg	116.6 ± 15.7	101.4 ± 15.4	<0.01
Diastolic blood pressure, mmHg	68.1 ± 10.9	63.2 ± 11.5	0.09
Laboratory findings			
Haemoglobin level, g/dL	13.0 ± 2.3	12.1 ± 2.0	0.10
eGFR, mL/min/1.73m ²	62.0 ± 23.6	49.9 ± 20.1	<0.05
BNP, pg/mL	174 (83–310) (n = 36)	634 (324–1300) (n = 28)	<0.01
Hs-cTnT, ng/mL	0.04 (0.03–0.07) (n = 32)	0.10 (0.07–0.18) (n = 28)	<0.01
C-reactive protein, mg/L	0.14 (0.06–0.25)	0.15 (0.05–0.65)	0.36
Difference FLC	257 (72–716) (n = 35)	419 (192–1195) (n = 17)	0.25
Electrocardiographic findings			
Low voltage	12 (34) (n = 35)	18 (62) (n = 29)	<0.05
Pseudo MI pattern	6 (17) (n = 35)	12 (41) (n = 29)	<0.05
CRBBB	4 (11) (n = 35)	3 (10) (n = 29)	0.89
Conventional echocardiographic findings			
LAVI, mL/m ²	49.0 ± 20.8	58.6 ± 23.1	0.08
IVSTd, mm	13.2 ± 2.0	14.3 ± 2.9	0.07
LVPWTD, mm	13.0 ± 2.2	13.7 ± 2.1	0.21
LVEF, %	60.1 ± 7.9	53.7 ± 10.1	<0.01
E/A	1.44 ± 1.21 (n = 33)	1.92 ± 1.36 (n = 25)	0.16
E/e' ratio	18.5 ± 7.8	24.7 ± 11.0	<0.05
RVFAC, %	29.6 ± 7.1	21.7 ± 8.7	<0.01
AS (%)	1 (3)	0 (0)	0.37
MR (%)	1 (3)	7 (24)	<0.01
TR (%)	1 (3)	3 (10)	0.21
Two-dimensional speckle tracking echocardiographic findings			
LV-GLS, %	11.7 ± 3.9	8.9 ± 4.2	<0.01
LASr, %	14.09 ± 8.32	9.06 ± 7.28	<0.05
pLASRr, S ⁻¹	0.58 ± 0.31	0.40 ± 0.25	<0.05
pLASRcd, S ⁻¹	0.45 ± 0.30 (n = 27)	0.41 ± 0.24 (n = 17)	0.61
pLASRct, S ⁻¹	0.51 ± 0.25 (n = 25)	0.33 ± 0.23 (n = 17)	<0.05
RV-GLS, %	16.8 ± 4.0	12.0 ± 5.1	<0.01
RVFWLS, %	20.2 ± 5.2	14.4 ± 5.9	<0.01
Cardiac treatment			
RAS inhibitor, n (%)	9 (25)	10 (34)	0.40

Continued

Table 1 Continued

	Event-free group (n = 36)	All-cause death group (n = 29)	P-value
MRA, n (%)	7 (19)	13 (45)	<0.05
Beta blocker, n (%)	5 (14)	7 (24)	0.29
Diuretic, n (%)	22 (61)	23 (79)	0.11
Haematological treatment			
Bortezomib, n (%)	15 (42)	6 (21)	0.07
Daratumumab, n (%)	30 (83)	6 (21)	<0.01

The P values were obtained by student's *t*-test, Mann–Whitney *U* test, or χ^2 test.

AS, aortic stenosis; BNP, B-type natriuretic peptide; CRBBB, complete right bundle branch block; eGFR, estimated glomerular filtration rate; FLC, free light chain; hs-cTnT, high sensitivity cardiac troponin T; GLS, global longitudinal strain; ICD, implantable cardioverter defibrillator; IVSTd, interventricular septal thickness in diastole; LV, left ventricle; LAVI, left atrial volume index; LVPWTd, left ventricular posterior wall thickness in diastole; LVEF, left ventricular ejection fraction; LASr, left atrial strain during reservoir phase; MI, myocardial infarction; MRA, mineralocorticoid receptor antagonist; MR, mitral regurgitation; pLASRr, peak strain rate during reservoir phase; pLASRcd, peak strain rate during conduit phase; pLASRct, peak strain rate during contraction phase; RV, right ventricle; RVFWLS, right ventricle free wall longitudinal strain; RAS, renin angiotensin system; RVFAC, right ventricular fractional area change; TR, tricuspid regurgitation.

Conventional echocardiographic measurements

TTE was performed in patients in a stable condition using the Vivid E95 or 7 (GE Vingmed, Horten, Norway), Aplio 500 (Canon Medical Systems Corp., Otawara, Tochigi, Japan), and Epiq 7G (Philips, Bothell, WA, USA), which were equipped with a 2.5-MHz phased-array transducer. Conventional echocardiography was performed according to the recommendations of the American Society of Echocardiography (ASE) and the European Association of Cardiovascular Imaging.^{17,18} LV wall thickness was acquired in the parasternal long-axis view. LV ejection fraction (LVEF) and LA volume index were calculated using a modified Simpson's method. Peak early diastolic velocity of LV inflow (E velocity), late atrial diastolic velocity of LV inflow (A velocity), and peak early diastolic velocity on the septal corner of the mitral annulus (e') were measured in the apical four-chamber view. Moderate or severe valvular diseases according to ASE guideline¹⁹ were defined as valvular diseases in this study. To minimize bias, the echocardiography reviewers were blinded to the patients' clinical history and data.

Two-dimensional speckle-tracking echocardiography

Two-dimensional speckle-tracking echocardiography was performed by one operator (first operator) who was blinded to the clinical data and who was different from the operator who performed the conventional echocardiography. Two-dimensional speckle-tracking echocardiography was performed using Cardiac Performance Analysis (2D-CPA): a manual vendor-independent measurement package (TomTec-Arena, TomTec Imaging Systems, Unterschleissheim, Germany). To assess the RVLS, we evaluated the average value of the longitudinal peak systolic strain only from the free wall [RV free wall LS (RVFWLS)] and from the free wall and the septal wall of the RV [RV global LS (RV-GLS)] in the RV focused apical four-chamber view²⁰ (Figure 2). To assess the LV strain, the LS, calculated from the echocardiography images in the four-chamber, three-chamber, and two-chamber views, was determined in 16 segments of the left ventricle in accordance with the ASE guidelines.¹⁷ The LV global LS (LV-GLS) was calculated as the average LS of these 16 segments. To assess LA strain, the regional strain and strain rate were determined in three segments (septal, roof, and lateral) obtained from echocardiographic images in the four-chamber apical view according to our previous report.^{21,22} To evaluate LA strain components, the zero-strain reference was defined at end-diastole. LA reservoir function was estimated using LA strain during the reservoir phase (LASr) and the peak LA strain rate during the reservoir phase (pLASRr) during the ventricular systole phase, which represents LA filling during LV systole. LA conduit function was estimated using the peak LA strain rate during the conduit phase (pLASRcd) during the LV diastole phase. In contrast, LA pump function was estimated using the peak LA strain rate during the contraction phase

(pLASRct) during the LV diastole phase.^{20,23} Strain and strain rate are described in absolute values. For assessment of intraobserver variability, the first operator reevaluated RV-GLS measurements from 20 patients 1 month after the initial calculation. For assessment of inter-observer variability, the RV-GLS measurements from 20 patients were paired to the measurement of another operator (second operator). The intra-observer and inter-observer variabilities were assessed using the intra-class correlation coefficient (ICC). Analysis of the intra-observer and inter-observer showed good correlations for RV-GLS measurements [mean ICC, 0.86; 95% confidence interval (CI), 0.69–0.94 and mean ICC, 0.83; 95% CI, 0.61–0.93, respectively].

Data collection

For patients receiving chemotherapy, laboratory examination, electrocardiogram, and TTE were performed before starting chemotherapy. Mortality was identified by a search of the medical records and confirmed by a questionnaire and direct contact via a telephone interview of the patient or, if deceased, a family member. The confirmation data were in July 2022.

Statistical analysis

Detailed statistical analysis is available in the [Supplementary material online](#).

Results

Diagnosis of AL cardiac amyloidosis

Among the 65 enrolled patients, 11 patients underwent endomyocardial biopsy, of whom 10 patients had AL amyloid deposition in the heart. In the other 55 patients, AL amyloid deposition was confirmed in other tissues (skin or abdominal fat pad, *n* = 23; gastrointestinal tract, *n* = 28; kidney, *n* = 9; other tissues, *n* = 5). Cardiac amyloidosis was defined according to amyloid deposition in the myocardium (*n* = 10) and/or typical findings of CMR (*n* = 36). Twenty-seven patients were defined as AL cardiac amyloidosis by echocardiography (IVSTd >12 mm) and AL amyloid deposition in non-cardiac tissues.

Comparison of clinical characteristics between all-cause death and survival groups

During a median follow-up of 359 days (interquartile range, 146–1287 days), 29 deaths occurred (heart failure, *n* = 15; out-of-hospital sudden death, *n* = 3; ventricular arrhythmia, *n* = 2; infection, *n* = 2; renal failure,

Table 2 Univariate Cox proportional hazards model for all-cause death

	Univariate analysis	
	HR (95% CI)	P-value
Age per 1 year	1.05 (1.00–1.09)	<0.05
Male sex/yes	0.87 (0.40–1.87)	0.71
Body mass index per 1 kg/m ²	0.96 (0.87–1.05)	0.32
Hypertension/yes	0.55 (0.23–1.28)	0.17
Diabetes mellitus/yes	0.45 (0.11–1.90)	0.28
Dyslipidaemia/yes	0.68 (0.26–1.79)	0.44
Atrial fibrillation/yes	1.43 (0.54–3.77)	0.47
Current smoking/yes	0.81 (0.11–5.99)	0.83
Haemoglobin level per 1 g/dL	0.91 (0.78–1.06)	0.23
Ln TnT per 1	2.00 (1.34–2.98)	<0.01
Ln BNP per 1	3.12 (2.00–4.88)	<0.01
eGFR per 1 mL/min/1.73 m ²	0.98 (0.97–1.00)	<0.05
difference FLC per 1	1.00 (1.00–1.00)	0.25
Stage I/yes	0.74 (0.22–2.45)	0.62
Stage II/yes	0.25 (0.06–1.06)	0.06
Stage IIIa/yes	0.50 (0.22–1.11)	0.09
Stage IIIb/yes	9.38 (4.09–21.56)	<0.01
Low voltage QRS in electrocardiography/yes	1.95 (0.92–4.13)	0.08
Pseudo MI pattern/yes	2.87 (1.36–6.06)	<0.01
LAVI per 1 mL/m ²	1.01 (1.00–1.03)	0.09
IVSTd per 1 mm	1.20 (1.03–1.39)	<0.05
LVPWTd per 1 mm	1.14 (0.97–1.33)	0.11
LVEF per 1%	0.95 (0.91–0.98)	<0.01
E/e' ratio per 1	1.05 (1.01–1.08)	<0.01
RVFAC per 1%	0.91 (0.87–0.95)	<0.01
Mitral regurgitation/yes	5.51 (2.28–13.30)	<0.05
Tricuspid regurgitation/yes	3.19 (0.95–10.72)	0.10
LV-GLS per 1%	0.83 (0.75–0.92)	<0.01
LASr per 1%	0.91 (0.86–0.98)	<0.01
pLASRr per 1	0.11 (0.19–0.60)	<0.05
pLASRcd per 1	0.39 (0.06–2.74)	0.35
pLASRct per 1	0.05 (0.00–0.57)	<0.05
RV-GLS per 1%	0.83 (0.76–0.89)	<0.01
RVFWLS per 1%	0.88 (0.83–0.93)	<0.01
RAS inhibitor/yes	1.36 (0.63–2.93)	0.43
MRA/yes	2.48 (1.18–5.19)	<0.05
Beta blocker/yes	2.07 (0.87–4.90)	0.10
Diuretics/yes	2.03 (0.83–5.00)	0.12
Bortezomib/yes	0.36 (0.14–0.90)	<0.05
Daratumumab/yes	0.11 (0.44–0.27)	<0.01

P value was obtained by the univariate Cox hazard analyses model.

$n = 2$; general weakness, $n = 2$; intestinal perforation, $n = 1$; multiple myeloma, $n = 1$; and unknown cause, $n = 1$). [Table 1](#) shows the clinical characteristics in the all-cause death group and the survival group. The rate of stage II was significantly lower, and the rate of stage IIIb was significantly higher in the all-cause death group than in the survival group. Among the laboratory findings, estimated glomerular filtration ratio

(eGFR) was significantly lower, and BNP and hs-TnT were significantly higher in the all-cause death group than in the survival group. Among the conventional echocardiographic findings, the LVEF and RV fractional area change (RVFAC) were significantly lower, and the E/e' ratio and the rate of mitral regurgitation (MR) were significantly higher in the all-cause death group than in the survival group. Among the two-dimensional speckle-tracking echocardiographic findings, LV-GLS, LASr, pLASRr, pLASRct, RV-GLS, and RVFWLS were significantly lower in the all-cause death group than in the survival group.

Cox proportional hazard analysis for all-cause death

As shown in [Table 2](#), the univariate Cox proportional hazard analysis showed that 20 variables were significant predictors of all-cause death: age, lnTnT, lnBNP, eGFR, stage IIIb, pseudo myocardial infarction pattern, IVSTd, LVEF, E/e' ratio, RVFAC, MR, LV-GLS, LASr, pLASRr, pLASRct, RV-GLS, RVFWLS, mineralocorticoid receptor antagonist use, bortezomib use, and daratumumab use. Considering the internal correlation and the number of patients in our study, we created five models to perform multivariable Cox proportional hazard analysis ([Table 3](#)). RV-GLS was significantly and independently associated with all-cause death after adjusting for RVFAC and RVFWLS (Model 1), LV-GLS and LASr (Model 2), conventional prognostic risk factors (Model 3), conventional echocardiographic findings (Model 4), and medications (Model 5).

ROC analysis for all-cause death

Receiver operating characteristic (ROC) analysis was performed to determine the optimal RV-GLS cut-off value for predicting all-cause death in patients with cardiac AL amyloidosis. As shown in [Figure 3](#), the area under the curve of RV-GLS for all-cause death was 0.774. We also found that the best cut-off value of RV-GLS was 14.5% (sensitivity, 75%; specificity, 72%).

Follow-up of patients with high and low rv-GLS values

We divided the patients into two groups using the best cut-off value of RV-GLS estimated by the ROC analysis: the high RV-GLS group ($\geq 14.5\%$, $n = 35$) and low RV-GLS group ($< 14.5\%$, $n = 30$). Kaplan–Meier analysis demonstrated a significantly higher risk of all-cause death in patients with high than with low RV-GLS ($P < 0.01$ by log-rank test) ([Figure 4](#)).

Next, we divided the patients into two groups: the daratumumab-based treatment group and non-daratumumab group. In the daratumumab-based treatment group, Kaplan–Meier analysis demonstrated a significantly higher risk of all-cause death in patients with low than high RV-GLS ($P < 0.05$; see [Supplementary material online, Figure S1A](#)). Even in the non-daratumumab group, patients with low RV-GLS had a significantly higher risk of all-cause death than patients with high RV-GLS ($P < 0.01$; see [Supplementary material online, Figure S1B](#)).

Discussion

The present study revealed the usefulness of RV-GLS by two-dimensional speckle-tracking echocardiography to predict all-cause death in patients with AL cardiac amyloidosis.

LV-GLS is a strong and independent predictor of outcomes in patients with AL amyloidosis.^{24–26} LALS and RVLS are also important prognostic predictors in patients with AL amyloidosis.^{27–31} However, these studies did not evaluate the superiority between RV, LV, and LA strain in patients with AL cardiac amyloidosis. In our present study,

Table 3 Multivariable Cox proportional hazards model for all-cause death

	Model 1		Model 2		Model 3		Model 4		Model 5	
	HR (95% CI)	P-value	HR (95% CI)	P-value	HR (95% CI)	P-value	HR (95% CI)	P-value	HR (95% CI)	P-value
RVFAC per 1%	0.97 (0.90–1.04)	0.33	—	—	—	—	—	—	—	—
RVFWLS per 1%	1.13 (0.91–1.40)	0.26	—	—	—	—	—	—	—	—
LV-GLS per 1%	—	—	0.94 (0.82–1.08)	0.40	—	—	—	—	—	—
LASr per 1%	—	—	0.98 (0.92–1.03)	0.42	—	—	—	—	—	—
RV-GLS per 1%	0.74 (0.56–0.98)	<0.05	0.85 (0.77–0.94)	<0.01	—	—	—	—	—	—
Age per 1 year	1.01 (0.96–1.07)	0.65	—	—	—	—	—	—	—	—
eGFR per 1 mL/min/1.73m ²	0.99 (0.96–1.07)	0.20	—	—	—	—	—	—	—	—
Stage IIIb	4.36 (0.69–5.01)	<0.01	—	—	—	—	—	—	—	—
IVSTd/1mm	—	—	1.19 (0.97–1.45)	0.09	—	—	—	—	—	—
E/e'/1	—	—	1.00 (0.95–1.04)	0.84	—	—	—	—	—	—
Mitral regurgitation/yes	—	—	10.77 (3.29–35.21)	<0.01	—	—	—	—	—	—
LVEF/1%	—	—	1.011 (0.96–1.07)	0.68	—	—	—	—	—	—
Bortezomib/yes	—	—	—	—	—	—	0.40 (0.15–1.12)	0.08	—	—
Daratumumab/yes	—	—	—	—	—	—	0.10 (0.04–0.27)	<0.01	—	—
MRA/yes	—	—	—	—	—	—	1.35 (0.57–3.25)	0.50	—	—
RV-GLS/1%	0.89 (0.80–1.00)	<0.05	0.82 (0.75–0.91)	<0.01	—	—	0.88 (0.82–0.95)	<0.01	—	—

P-value was obtained by the multivariate Cox hazard analysis.

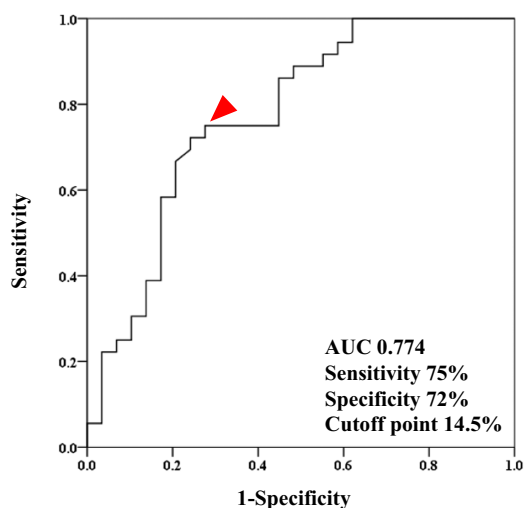


Figure 3 Receiver operator characteristic curve analysis of right ventricular global longitudinal strain for predicting all-cause death. AUC, area under the curve.

we revealed the superiority of RV-GLS over LV-GLS and LALS to predict all-cause mortality in these patients.

Accumulated evidence has revealed the importance of evaluating the RV function in patients with heart failure.³² In patients with AL cardiac amyloidosis, the RV is affected by not only direct amyloid deposition

but also LV and LA dysfunction. For instance, LV dysfunction secondarily aggravates RV dysfunction because of pulmonary venous hypertension, ventricular interdependence, neurohormonal interactions, and myocardial ischaemia of the RV.³³ In addition, LA dysfunction and enlargement due to pressure and volume overload cause structural changes in the other chambers, including concomitant tricuspid annulus dilatation, increased mobility of the tricuspid leaflets, and tricuspid regurgitation,^{34,35} which would result in RV remodelling and affect RV longitudinal function. We speculate that the RV-GLS could provide greater prognostic power even compared to LV-GLS and LALS in patients with cardiac AL amyloidosis, because RV dysfunction might reflect the burden of LV dysfunction, LA dysfunction, and amyloidosis deposition as a whole.

Binder *et al.*³⁶ showed that RV strain was not significant in AL amyloidosis, whereas LV-GLS was superior in AL amyloidosis, and this result is not in line with ours. Binder *et al.* used RVFWLS as RV strain, which was thought to be important difference from our present study. Our present study compared RV-GLS and RVFWLS and revealed that RV-GLS, but not RVFWLS, was independently associated with the prognosis in patients with AL cardiac amyloidosis. We previously reported the superiority of RV-GLS over RVFWLS as a prognostic factor in patients with transthyretin amyloid cardiomyopathy.¹⁴ Thus, we considered RV-GLS may be an important prognostic factor in patients with any phenotype of amyloid cardiomyopathy. RVFWLS is associated with RV stroke volume,³⁷ and RV-GLS is more closely associated with LV systolic function than is RVFWLS,³⁸ because RV-GLS is composed of RVFWLS and the septal wall longitudinal strain. Therefore, RV-GLS was thought to be affected by not only RV but also LV, which might be the reason why RV-GLS had a stronger effect than RVFWLS on the prognosis in patients with cardiac amyloidosis.

Diagnostic delay in AL amyloidosis leads to advanced multi-organ involvement and poor prognosis.³⁹ The addition of daratumumab to

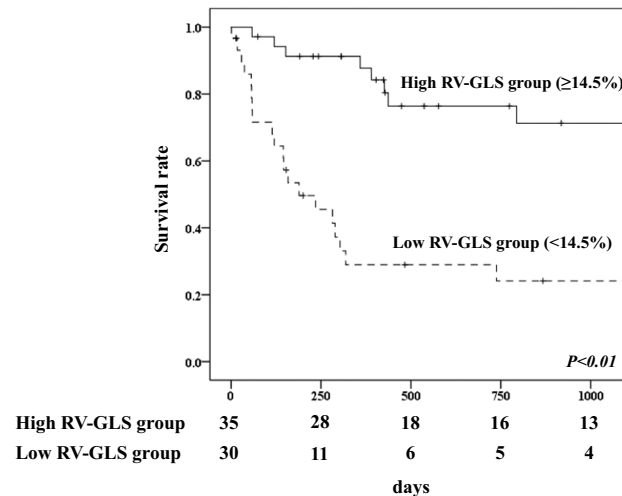


Figure 4 Kaplan–Meier curves of all-cause death in patients with immunoglobulin light-chain amyloidosis cardiac amyloidosis with high or low right ventricular global longitudinal strain.

classical medical therapy was recently shown to be associated with survival free from major organ deterioration or haematologic progression in patients with newly diagnosed AL amyloidosis.⁴⁰ Therefore, daratumumab combination therapy represents an important emerging first-line treatment option for patients with systemic AL amyloidosis. However, few data are available regarding prognostic echocardiographic factors in patients with daratumumab therapy. Our study revealed that RV-GLS was independently associated with all-cause mortality even after adjusting for administration of daratumumab therapy. In addition, the low RV-GLS group had a significantly higher mortality rate than the high RV-GLS group among patients receiving daratumumab therapy. These results indicate that RV-GLS is an important prognostic factor even in patients with daratumumab therapy. Thus, daratumumab therapy should be started in the early stage of AL cardiac amyloidosis, when RV function is fully preserved.

Study limitations

This study had several limitations. First, this was a retrospective single-centre study that included a relatively small number of patients with AL cardiac amyloidosis. Second, echocardiographic images were obtained using several ultrasound machines. We performed the two-dimensional speckle-tracking echocardiography analysis using vendor-independent software (TomTec Image-Arena™). Although significant correlations have been shown in the LS values analysed using vendor-independent software for paired images obtained from different ultrasound machines,⁴¹ inter-machine variability may have still affected our study results. In addition, medical therapy is thought to have a significant impact on the strain value. However, we did not consider baseline medical therapy in our present study, which may have some effect on our study results. Third, several patients were diagnosed with AL cardiac amyloidosis before the RV-focused apical four-chamber view was recommended. Therefore, we had no choice but to use the apical four-chamber view to evaluate RV-GLS in these patients. In addition, e' lateral line was not measured in several patients because they were diagnosed with AL cardiac amyloidosis before e' lateral line was recommended. Therefore, we used only e' septal line to evaluate LV diastolic function in our present study. Fourth, we did not evaluate RV function data obtained by CMR because several patients did not undergo CMR. Fifth, we did not clarify the term of medical treatment,

including daratumumab therapy. In our present study, 27 patients were defined as cardiac amyloidosis by echocardiography alone. It cannot be denied that LV hypertrophy in these patients was caused by other reasons such as arterial hypertension. This is one of the other important limitations.

Despite these limitations, the present study demonstrated the importance of RV function estimated by two-dimensional strain analysis compared to LVLS and LALS in patients with AL cardiac amyloidosis. We believe that our results have significant value in the clinical setting. In these days, the effect of three-dimensional speckle tracking imaging on RV strain in patients with AL amyloidosis was reported.⁴² Thus, we should evaluate the prognostic impact of RV strain by three-dimensional speckle tracking imaging in patients with AL cardiac amyloidosis in the future.

Conclusion

RV-GLS has prognostic value in patients with AL cardiac amyloidosis and provides greater prognostic power than LV-GLS and LALS. Further prospective studies with more patients are needed to validate our results.

Lead author biography



Hiroki Usuku is a specialist in cardiovascular medicine and echocardiography. He is an assistant professor of central laboratory medicine in Kumamoto University Hospital. He has Board Certified Member of the Japanese Circulation Society, Fellow of Japanese Society of Internal Medicine, and Board Certified Fellow of the Japan Society of Ultrasonics in Medicine. He specializes in conducting research on echocardiographic finding of amyloid cardiomyopathy.

Data availability

The data underlying the research results described in this paper are not publicly available due to the privacy of research participants.

Supplementary material

Supplementary material is available at *European Heart Journal Open* online.

Acknowledgements

We thank Angela Morben, DVM, ELS, from Edanz (<https://jp.edanz.com/ac>) for editing a draft of this manuscript.

Funding

This study was supported in part by Grants-in-Aid for Scientific Research (grant number 20K17087) from the Ministry of Education, Culture, Sports, Science and Technology of Japan to D.S.; Grant-in-Aid for Scientific Research (grant number 20K08476) from Japan Society for the Promotion of Science to H.U.; and research grant from Pfizer Japan Incorporated to H.U.

Conflict of interest: None declared.

Ethics approval

This study was approved by the institutional review board and ethics committee of Kumamoto University (reference number: 1588).

References

- Kitaoka H, Izumi C, Izumiya Y, Inomata T, Ueda M, Kubo T, Izumi C, Izumiya Y, Inomata T, Ueda M, Kubo T, Koyama J, Sano M, Sekijima Y, Tahara N, Tsukada N, Tsujita K, Tsutsui H, Tomita T, Amano M, Endo J, Okada A, Oda S, Takashio S, Baba Y, Misumi Y, Yazaki M, Anzai T, Ando Y, Isobe M, Kimura T, Fukuda K. JCS 2020 guideline on diagnosis and treatment of cardiac amyloidosis. *Circ J* 2020;**84**:1610–1671.
- Palladini G, Milani P, Merlini G. Management of AL amyloidosis in 2020. *Blood* 2020;**136**:2620–2627.
- Kyle RA, Greipp PR, O'Fallon WM. Primary systemic amyloidosis: multivariate analysis for prognostic factors in 168 cases. *Blood* 1986;**68**:220–224.
- Milani P, Merlini G, Palladini G. Light chain amyloidosis. *Mediterr J Hematol Infect Dis* 2018;**10**:e2018022.
- Gillmore JD, Wechalekar A, Bird J, Cavenagh J, Hawkins S, Kazmi M, Lachmann HJ, Hawkins PN, Pratt G. Guidelines on the diagnosis and investigation of AL amyloidosis. *Br J Haematol* 2015;**168**:207–218.
- Brenner DA, Jain M, Pimentel DR, Wang B, Connors LH, Skinner M, Apstein CS, Liao R. Human amyloidogenic light chains directly impair cardiomyocyte function through an increase in cellular oxidant stress. *Circ Res* 2004;**94**:1008–1010.
- Cueto-Garcia L, Reeder GS, Kyle RA, Wood DL, Seward JB, Naessens J, Offord KP, Greipp PR, Edwards WD, Tajik AJ. Echocardiographic findings in systemic amyloidosis: spectrum of cardiac involvement and relation to survival. *J Am Coll Cardiol* 1985;**6**:737–743.
- Kristen AV, Perz JB, Schonland SO, Hegenbart U, Schnabel PA, Kristen JH, Goldschmidt H, Katus HA, Dengler TJ. Non-invasive predictors of survival in cardiac amyloidosis. *Eur J Heart Fail* 2007;**9**:617–624.
- Mohty D, Damy T, Cosnay P, Echahidi N, Casset-Senon D, Virot P, Jaccard A. Cardiac amyloidosis: updates in diagnosis and management. *Arch Cardiovasc Dis* 2013;**106**:528–540.
- Phelan D, Collier P, Thavendiranathan P, Popovic ZB, Hanna M, Plana JC, Marwick TH, Thomas JD. Relative apical sparing of longitudinal strain using two-dimensional speckle-tracking echocardiography is both sensitive and specific for the diagnosis of cardiac amyloidosis. *Heart* 2012;**98**:1442–1448.
- Falk RH. Diagnosis and management of the cardiac amyloidoses. *Circulation* 2005;**112**:2047–2060.
- Falk RH, Quarta CC. Echocardiography in cardiac amyloidosis. *Heart Fail Rev* 2015;**20**:125–131.
- Amundsen BH, Helle-Valle T, Edvardsen T, Torp H, Crosby J, Lyseggen E, Støylen A, Ihlen H, Lima JAC, Smiseth OA, Slørdahl SA. Noninvasive myocardial strain

- measurement by speckle tracking echocardiography: validation against sonomicrometry and tagged magnetic resonance imaging. *J Am Coll Cardiol* 2006;**47**:789–793.
- Usuku H, Takashio S, Yamamoto E, Yamada T, Egashira K, Morioka M, Nishi Masato, Komorita Takashi, Oike Fumi, Tabata Noriaki, Ishii Masanobu, Yamanaga Kenshi, Fujisue Koichiro, Sueta Daisuke, Arima Yuichiro, Araki Satoshi, Oda Seitaro, Misumi Yohei, Kawano Hiroaki, Matsushita Kenichi, Ueda Mitsuharu, Matsui Hiroataka, Tsujita Kenichi. Prognostic value of right ventricular global longitudinal strain in transthyretin amyloid cardiomyopathy. *J Cardiol* 2022;**80**:56–63.
 - Lyon AR, López-Fernández T, Couch LS, Asteggiano R, Aznar MC, Bergler-Klein J, Boriani G, Cardinale D, Cordoba R, Cosyns B, Cutter DJ, de Azambuja E, de Boer RA, Dent SF, Farmakis D, Gevaert SA, Gorog DA, Herrmann J, Lenihan D, Moslehi J, Moura B, Salinger SS, Stephens R, Suter TM, Szmit S, Tamargo J, Thavendiranathan P, Tocchetti CG, van der Meer P, van der Pal HJH, Lancellotti P, Thuny F, Abdelhamid M, Aboyans V, Aleman B, Alexandre J, Barac A, Borger MA, Casado-Arroyo R, Cautela J, Čelutkienė J, Cikes M, Cohen-Solal A, Dhiman K, Ederhy S, Edvardsen T, Fauchier L, Fradley M, Grapsa J, Halvorsen S, Heuser M, Humbert M, Jaarsma T, Kahan T, Konradi A, Koskinas KC, Kotecha D, Ky B, Landmesser U, Lewis BS, Linhart A, Lip GYH, Löchen M-L, Malaczynska-Rajpold K, Metra M, Mindham R, Moonen M, Neilan TG, Nielsen JC, Petronio A-S, Prescott E, Rakisheva A, Salem J-E, Savarese G, Sitges M, Berg Jt, Touyz RM, Tycinska A, Wilhelm M, Zamorano JL, Laredj N, Zelveian P, Rainer PP, Samadov F, Andruschuk U, Gerber BL, Selimović M, Kinova E, Samardzic J, Economides E, Pudi R, Nielsen KM, Kafay TA, Vettus R, Tuohinen S, Ederhy S, Pagava Z, Rassaf T, Briassoulis A, Czuriga D, Andersen KK, Smyth Y, Iakobishvili Z, Parrini I, Rakisheva A, Pruthi EP, Mirrahimov E, Kalejs O, Skouri H, Benjamin H, Žaliaduonytė D, Iovino A, Moore AM, Bursacovschi D, Benyass A, Manintveld O, Bosevski M, Gulati G, Leszek P, Fiuza M, Jurcut R, Vasyuk Y, Foscoli M, Simic D, Slanina M, Lipar L, Martin-Garcia A, Hübbert L, Kurmann R, Alayed A, Abid L, Zorkun C, Nesukay E, Manisty C, Srojdinova N. 2022 ESC guidelines on cardio-oncology developed in collaboration with the European Hematology Association (EHA), the European Society for Therapeutic Radiology and Oncology (ESTRO) and the International Cardio-Oncology Society (IC-OS). *Eur Heart J* 2022;**43**:4229–4361.
 - Lillenes B, Ruberg FL, Mussinelli R, Doros G, Sancharawala V. Development and validation of a survival staging system incorporating BNP in patients with light chain amyloidosis. *Blood* 2019;**133**:215–223.
 - Lang RM, Badano LP, Mor-Avi V, Afilalo J, Armstrong A, Ernande L, Flachskampf FA, Foster E, Goldstein SA, Kuznetsova T, Lancellotti P, Muraru D, Picard MH, Rietzschel ER, Rudski L, Spencer KT, Tsang W, Voigt J-U. Recommendations for cardiac chamber quantification by echocardiography in adults: an update from the American Society of Echocardiography and the European Association of Cardiovascular Imaging. *J Am Soc Echocardiogr* 2015;**28**:1–39.e14.
 - Nagueh SF, Smiseth OA, Appleton CP, Byrd BF III, Dokainish H, Edvardsen T, Flachskampf FA, Gillebert TC, Klein AL, Lancellotti P, Marino P, Oh JK, Popescu BA, Waggoner AD. Recommendations for the evaluation of left ventricular diastolic function by echocardiography: an update from the American Society of Echocardiography and the European Association of Cardiovascular Imaging. *J Am Soc Echocardiogr* 2016;**29**:277–314.
 - Zoghbi WA, Adams D, Bonow RO, Enriquez-Sarano M, Foster E, Grayburn PA, Hahn RT, Han Y, Hung J, Lang RM, Little SH, Shah DJ, Shernan S, Thavendiranathan P, Thomas JD, Weissman NJ. Recommendations for noninvasive evaluation of native valvular regurgitation: a report from the American Society of Echocardiography developed in collaboration with the society for cardiovascular magnetic resonance. *J Am Soc Echocardiogr* 2017;**30**:303–371.
 - Badano LP, Kollas TJ, Muraru D, Abraham TP, Aurigemma G, Edvardsen T, D'Hooge J, Donal E, Fraser AG, Marwick T, Mertens L, Popescu BA, Sengupta PP, Lancellotti P, Thomas JD, Voigt J-U, Prater D, Chono T, Mumm B, Houle H, Healthineers S, Hansen G, Abe Y, Pedri S, Delgado V, Gimelli A, Cosyns B, Gerber B, Flachskampf F, Haugaa K, Galderisi M, Cardim N, Kaufmann P, Masci PG, Marsan NA, Rosca M, Cameli M, Sade LE. Standardization of left atrial, right ventricular, and right atrial deformation imaging using two-dimensional speckle tracking echocardiography: a consensus document of the EACVI/ASE/industry task force to standardize deformation imaging. *Eur Heart J Cardiovasc Imaging* 2018;**19**:591–600.
 - Oike F, Usuku H, Yamamoto E, Yamada T, Egashira K, Morioka M, Nishi M, Komorita T, Hirakawa K, Tabata N, Yamanaga K, Fujisue K, Hanatani S, Sueta D, Arima Y, Araki S, Takashio S, Oda S, Misumi Y, Kawano H, Matsushita K, Ueda M, Matsui H, Tsujita K. Prognostic value of left atrial strain in patients with wild-type transthyretin amyloid cardiomyopathy. *ESC Heart Fail* 2021;**8**:5316–5326.
 - Oike F, Usuku H, Yamamoto E, Marume K, Takashio S, Ishii M, Tabata N, Fujisue K, Yamanaga K, Sueta D, Hanatani S, Arima Y, Araki S, Oda S, Kawano H, Soejima H, Matsushita K, Ueda M, Fukui T, Tsujita K. Utility of left atrial and ventricular strain for diagnosis of transthyretin amyloid cardiomyopathy in aortic stenosis. *ESC Heart Fail* 2022;**9**:1976–1986.
 - Nochioka K, Quarta CC, Claggett B, Roca GQ, Rapezzi C, Falk RH, Solomon SD. Left atrial structure and function in cardiac amyloidosis. *Eur Heart J Cardiovasc Imaging* 2017;**18**:1128–1137.

24. Buss SJ, Emami M, Mereles D, Korosoglou G, Kristen AV, Voss A, Schellberg D, Zugck C, Galuschky C, Giannitsis E, Heegenbart U, Ho AD, Katus HA, Schonland SO, Hardt SE. Longitudinal left ventricular function for prediction of survival in systemic light-chain amyloidosis: incremental value compared with clinical and biochemical markers. *J Am Coll Cardiol* 2012;**60**:1067–1076.
25. Salinaro F, Meier-Ewert HK, Miller EJ, Pandey S, Sancharawala V, Berk JL, Seldin DC, Ruberg FL. Longitudinal systolic strain, cardiac function improvement, and survival following treatment of light-chain (AL) cardiac amyloidosis. *Eur Heart J Cardiovasc Imaging* 2017;**18**:1057–1064.
26. Barros-Gomes S, Williams B, Nhola LF, Grogan M, Maalouf JF, Dispenzieri A, Pelliikka PA, Villarraga HR. Prognosis of light chain amyloidosis with preserved LVEF: added value of 2D speckle-tracking echocardiography to the current prognostic staging system. *JACC Cardiovasc Imaging* 2017;**10**:398–407.
27. Tan Z, Yang Y, Wu X, Li S, Li L, Zhong L, Lin Q, Fei H, Liao P, Wang W, Liu H. Left atrial remodeling and the prognostic value of feature tracking derived left atrial strain in patients with light-chain amyloidosis: a cardiovascular magnetic resonance study. *Int J Cardiovasc Imaging* 2022;**38**:1519–1532.
28. Uzan C, Lairez O, Raud-Raynier P, Garcia R, Degand B, Christiaens LP, Rehman MB. Right ventricular longitudinal strain: a tool for diagnosis and prognosis in light-chain amyloidosis. *Amyloid* 2018;**25**:18–25.
29. Huntjens PR, Zhang KW, Soyama Y, Karpalioti M, Lenihan DJ, Gorcsan J III. Prognostic utility of echocardiographic atrial and ventricular strain imaging in patients with cardiac amyloidosis. *JACC Cardiovasc Imaging* 2021;**14**:1508–1519.
30. Cappelli F, Porciani MC, Bergesio F, Perlini S, Attanà P, Moggi Pignone A, Salinaro F, Musca F, Padeletti L, Perfetto F. Right ventricular function in AL amyloidosis: characteristics and prognostic implication. *Eur Heart J Cardiovasc Imaging* 2012;**13**:416–422.
31. Tjahjadi C, Fortuni F, Stassen J, Debonnaire P, Lustosa RP, Marsan NA, Delgado V, Baj JJ. Prognostic implications of right ventricular systolic dysfunction in cardiac amyloidosis. *Am J Cardiol* 2022;**173**:120–127.
32. Konstam MA, Kiernan MS, Bernstein D, Bozkurt B, Jacob M, Kapur NK, Kociol RD, Lewis EF, Mehra MR, Pagani FD, Raval AN, Ward C. Evaluation and management of right-sided heart failure: a scientific statement from the American Heart Association. *Circulation* 2018;**137**:e578–e622.
33. Haddad F, Doyle R, Murphy DJ, Hunt SA. Right ventricular function in cardiovascular disease, part II: pathophysiology, clinical importance, and management of right ventricular failure. *Circulation* 2008;**117**:1717–1731.
34. Katsi V, Raftopoulos L, Aggeli C, Vlaseros I, Felekos I, Tousoulis D, Stefanadis C, Kallikazaros I. Tricuspid regurgitation after successful mitral valve surgery. *Interact Cardiovasc Thorac Surg* 2012;**15**:102–108.
35. Utsunomiya H, Itabashi Y, Mihara H, Berdejo J, Kobayashi S, Siegel RJ, Shiota T. Functional tricuspid regurgitation caused by chronic atrial fibrillation: a real-time 3-dimensional transesophageal echocardiography study. *Circ Cardiovasc Imaging* 2017;**10**:e004897.
36. Binder C, Duca F, Stelzer PD, Nitsche C, Rettl R, Aschauer S, Kammerlander AA, Binder T, Agis H, Kain R, Hengstenberg C, Mascherbauer J, Bonderman D. Mechanisms of heart failure in transthyretin vs. light chain amyloidosis. *Eur Heart J Cardiovasc Imaging* 2019;**20**:512–524.
37. Leather HA, Ama' R, Missant C, Rex S, Rademakers FE, Wouters PF. Longitudinal but not circumferential deformation reflects global contractile function in the right ventricle with open pericardium. *Am J Physiol Heart Circ Physiol* 2006;**290**:H2369–H2375.
38. Hamada-Harimura Y, Seo Y, Ishizu T, Nishi I, Machino-Ohtsuka T, Yamamoto M, Sugano A, Sato K, Sai S, Obara K, Yoshida I, Aonuma K. Incremental prognostic value of right ventricular strain in patients with acute decompensated heart failure. *Circ Cardiovasc Imaging* 2018;**11**:e007249.
39. Palladini G, Sachchithanatham S, Milani P, Gillmore J, Foli A, Lachmann H, Basset M, Hawkins P, Merlini G, Wechalekar AD. A European collaborative study of cyclophosphamide, bortezomib, and dexamethasone in upfront treatment of systemic AL amyloidosis. *Blood* 2015;**126**:612–615.
40. Kastritis E, Palladini G, Minnema MC, Wechalekar AD, Jaccard A, Lee HC, Sancharawala V, Gibbs S, Mollee P, Venner CP, Lu J, Schönland S, Gatt ME, Suzuki K, Kim K, Cibeira MT, Beksac M, Libby E, Valent J, Hungria V, Wong SW, Rosenzweig M, Bumma N, Huart A, Dimopoulos MA, Bhutani D, Waxman AJ, Goodman SA, Zonder JA, Lam S, Song K, Hansen T, Manier S, Roeloffzen W, Jamrozjak K, Kwok F, Shimazaki C, Kim J-S, Crusoe E, Ahmadi T, Tran N, Qin X, Vasey SY, Tromp B, Schecter JM, Weiss BM, Zhuang SH, Vermeulen J, Merlini G, Comenzo RL. Daratumumab-based treatment for immunoglobulin light-chain amyloidosis. *N Engl J Med* 2021;**385**:46–58.
41. Nagata Y, Takeuchi M, Mizukoshi K, Wu VC, Lin FC, Negishi K, Nakatani S, Otsuji Y. Intervendor variability of two-dimensional strain using vendor-specific and vendor-independent software. *J Am Soc Echocardiogr* 2015;**28**:630–641.
42. Vitarelli A, Lai S, Petrucci MT, Gaudio C, Capotosto L, Mangieri E, Ricci S, Germanò G, De Sio S, Trusculli G, Vozella F, Pergolini MS, Giordano M. Biventricular assessment of light-chain amyloidosis using 3D speckle tracking echocardiography: differentiation from other forms of myocardial hypertrophy. *Int J Cardiol* 2018;**271**:371–377.